Journal of Intelligent & Fuzzy Systems xx (20xx) x–xx
DOI:10.3233/JIFS-190216
IOS Press



# Unscented Kalman filter for learning of a solar dryer and a greenhouse

José de Jesús Rubio*, Enrique Garcia, Genaro Ochoa, Israel Elias, David Ricardo Cruz, Ricardo Balcazar, Jesus Lopez and Juan Francisco Novoa
*Sección de Estudios de Posgrado e Investigación, ESIME Azcapotzalco, Instituto Politécnico Nacional, Av. de las Granjas no. 682, Col. Santa Catarina, México D.F., 02250, México*



**Abstract**. An unscented Kalman filter can be applied for the experimental learning of the solar dryer for oranges drying and the greenhouse for crop growth to know better the processes and to improve their performances. The contributions of this document are: a) an unscented Kalman filter is designed for the learning of nonlinear functions, b) the unscented Kalman filter is applied for the experimental learning of the two mentioned processes.

Keywords: Unscented Kalman filter, greenhouse, solar dryer, experimental learning

## 1. Introduction

Due to the population growth and the decrease of available spaces to treat food, it is raising the necessity to carry out research to improve some processes related to food: a solar dryer for oranges drying and a greenhouse for crop growth. Many agricultural products require a post-harvest drying process to properly preserve the products until they reach the consumer centers [1]. The use of greenhouses has become a measure taken for the controlled harvest of various vegetables [2]. Agricultural products offer the alternative to farmers when the price grows caused by overpopulation, and the learning is an important method in the current research of this issue.

The use of solar dryers, where products are directly exposed to the sun on the ground is one of oldest uses of solar energy and is still one of the agricultural processes most commonly used in many countries worldwide. Product quality is affected by the dust and insect contamination. In industrialized regions, the low cost of fuel allowed for several decades, the development of artificial drying processes on a large scale based on the use of fuels. In recent years, the shortage and price increase of fuel has sparked a new interest in the use of solar dryers, which tries to develop various techniques to solve the mentioned problems. Knowledge of solar radiation is essential to calculate various performance levels associated with solar power processes like solar dryers, solar water heaters and photovoltaic processes [3].

The employment of solar dryers through which dry air flows as an effect of natural convection can be an option for solving the problems of agricultural drying in small rural locations. These dryers can be constructed with simple materials and low skilled work, where the air flows by the pressure variations without an electric fan, and pressure variations in the air are caused by differences in temperature and humidity of the drying air and ambient air.

Several solar devices for drying food have been built and tested. In [4], a solar dryer is developed for vegetables by using natural convection to study the performance of drying in tomato and carrot, where a 50% saving in drying time is reported using a solar dryer at an average temperature of $60^oC$. In [5], the behavior of dried slices of lemon by using a solar

*Corresponding author. José de Jesús Rubio, Sección de Estudios de Posgrado e Investigación, ESIME Azcapotzalco, Instituto Politécnico Nacional, Av. de las Granjas no. 682, Col. Santa Catarina, México D.F., 02250, México. E-mail: rubio.josedejesus@gmail.com.

dryer combining a photovoltaic module and a dehumidifier process is studied to remove moisture in the fresh lemon slices; nevertheless, the photovoltaic module increases the total cost of drying by increasing the drying speed, results are compared to a hot air drying at 60°C.

For the control implementation of the main variables related to a greenhouse, it is necessary to have a model to represent the dynamics of the process. The model of [2, 6] is employed because it considers the most significant environmental aspects of a greenhouse.

There is some research about algorithms for the learning of nonlinear processes. In [7, 8], the deep learning method is studied. Machine learning approaches are discussed in [9–12]. In [13, 14], unsupervised learning techniques are addressed. Even than there are several algorithms for the learning of nonlinear processes, it should be interesting to study filters as one alternative for the learning in nonlinear processes because the filters could learn faster than other algorithms.

There is some research about filters for the learning of nonlinear processes. The extended Kalman filter is considered in [15–17]. In [18–20] the unscented Kalman filter is focused. It shows that the filters also have been highly studied for the learning of nonlinear processes. Consequently, a filter could be a good option for the learning of nonlinear processes.

The main difference between the extended Kalman filter and unscented Kalman filter is that the unscented Kalman filter can be designed by a deterministic procedure while the extended Kalman filter can be designed by a stochastic procedure. Hence, the unscented Kalman filter could be well applied to deterministic nonlinear processes while the extended Kalman filter could be well applied to stochastic nonlinear processes. Since this study is focused in deterministic nonlinear processes, the unscented Kalman filter is the best option.

In this document, the unscented Kalman filter is employed for the experimental learning of two processes by the next steps:

1. The unscented Kalman filter is applied for the experimental learning of nonlinear processes. The unscented Kalman filter as the same as the extended Kalman filter represent alternatives for the minimization of a cost function which could learn faster than other algorithms [15, 16].
2. The unscented Kalman filter is applied for the experimental learning of the next two processes: a solar dryer for oranges drying and a greenhouse for crop growth. a) A prototype of a solar dryer with a tracking process has been built and tested. Twenty-five drying tests are conducted from July to October 2015, where those tests are performed from 10:00 hours to 16:00 hours. b) A model of a greenhouse is presented and an approximation method is applied with real data from tests to validate the model and learning.

## 2. Approximation model

We consider the nonlinear model:

$$y_i = f(\mathbf{x}_i) \tag{1}$$

$\mathbf{x}_i = \begin{bmatrix} x_{1i} \; x_{2i} \; \dots \; x_{di} \end{bmatrix}^{\mathrm{T}}$ represents a vector of examples with size $d$, $\mathbf{x}_i$ also represents the inputs, $d$ represents the number of inputs, $y_i$ represents the output, $f(\cdot)$ represents a nonlinear function. $i$ represents the examples which vary from $i = 1$ to $i = m - 1$, and $m - 1$ represents the number of examples.

The regression model proposed to approximate the nonlinear model (1) is $\widehat{\mathbf{y}}_i = \mathbf{w}\mathbf{x}_i + b$ with examples from $i = 1$ to $i = m - 1$, $\mathbf{w} = \begin{bmatrix} w_0 \; w_1 \; w_2 \; \dots \; w_d \end{bmatrix}$ represents the weights and $\mathbf{x}_i = \begin{bmatrix} x_0 \; x_{1i} \; x_{2i} \; \dots \; x_{di} \end{bmatrix}^{\mathrm{T}}$ represents the examples. If $w_0 = b$ and $x_0 = 1$, then the regression model becomes to:

$$\widehat{\mathbf{y}}_i = \mathbf{w}\mathbf{x}_i \tag{2}$$

$\mathbf{w} = \begin{bmatrix} w_0 \; w_1 \; w_2 \; \dots \; w_d \end{bmatrix}$ represents the weights and $\mathbf{x}_i = \begin{bmatrix} x_0 \; x_{1i} \; x_{2i} \; \dots \; x_{di} \end{bmatrix}^{\mathrm{T}}$ represents the examples.

We define the error $e_i$ as:

$$e_i = \widehat{y}_i - y_i = \mathbf{w}\mathbf{x}_i - y_i \tag{3}$$

$y_i$ represents the output (1), $\widehat{y}_i$ represents the approximation of the regression model (2).

We define the cost $J$ as:

$$J = \sum_{i=0}^{m-1} e_i^2 \tag{4}$$

$e_i$ represents the error (3).

To reach the best approximation $\widehat{y}_i$ for the output $y_i$, we require the minimum of error $e_i^2$, we will find the weights $\mathbf{w}$ to reach the minimum of the cost $J$, we represent it as:

$$\frac{\partial J}{\partial \mathbf{w}} = 0 \tag{5}$$

We make operations to reach (5) as:

$$\begin{aligned}
&\frac{\partial J}{\partial \mathbf{w}} = \sum_{i=0}^{m-1} \frac{\partial J}{\partial e_i}\frac{\partial e_i}{\partial \mathbf{w}} = 0 \\
&\Rightarrow \sum_{i=0}^{m-1} 2e_i(\mathbf{x}_i) = 0 \\
&\Rightarrow \sum_{i=0}^{m-1} (\widehat{y}_i - y_i)(\mathbf{x}_i) = 0 \\
&\Rightarrow \sum_{i=0}^{m-1} (\mathbf{w}\mathbf{x}_i - y_i)(\mathbf{x}_i) = 0 \\
&\Rightarrow \mathbf{w}\sum_{i=0}^{m-1} \mathbf{x}_i^T\mathbf{x}_i = \sum_{i=0}^{m-1} y_i\mathbf{x}_i \\
&\Rightarrow \mathbf{w} = \left[\sum_{i=0}^{m-1} \mathbf{x}_i^T\mathbf{x}_i\right]^{-1} \sum_{i=0}^{m-1} y_i\mathbf{x}_i
\end{aligned} \tag{6}$$

We find the weights $\mathbf{w}$ as:

$$\mathbf{w} = \left[\sum_{i=0}^{m-1} \mathbf{x}_i^T\mathbf{x}_i\right]^{-1} \sum_{i=0}^{m-1} y_i\mathbf{x}_i \tag{7}$$

### 2.1. Unscented Kalman filter

We use the unscented Kalman filter to minimize the cost. We use small steps in the direction of the minimum of the cost.

To reach the unscented Kalman filter, we use the weights $\mathbf{w}$ of (7). We define the term $G_{m-1}$ as:

$$G_{m-1} = \sum_{i=0}^{m-1} \mathbf{x}_i^T\mathbf{x}_i \tag{8}$$

We substitute $G_{m-1}$ of (8) in (7) to reach the weights $\mathbf{w}$ in the iterations $m$ and $m+1$:

$$\begin{aligned}
\mathbf{w}_m &= G_{m-1}^{-1}\sum_{i=0}^{m-1} y_i\mathbf{x}_i \\
\mathbf{w}_{m+1} &= G_m^{-1}\sum_{i=0}^{m} y_i\mathbf{x}_i
\end{aligned} \tag{9}$$

We reach the next summation:

$$\sum_{i=0}^{m} y_i\mathbf{x}_i = \sum_{i=0}^{m-1} y_i\mathbf{x}_i + y_m\mathbf{x}_m \tag{10}$$

We make the mathematical operations, we get:

$$\begin{aligned}
\sum_{i=0}^{m} y_i\mathbf{x}_i &= \sum_{i=0}^{m-1} y_i\mathbf{x}_i + y_m\mathbf{x}_m \\
&= G_{m-1}\mathbf{w}_m + y_m\mathbf{x}_m \\
&= \left[G_{m-1}\mathbf{w}_m + y_m\mathbf{x}_m\right. \\
&\left.+\mathbf{x}_m^T\mathbf{x}_m\mathbf{w}_m - \mathbf{x}_m^T\mathbf{x}_m\mathbf{w}_m\right] \\
&= \left[\left(G_{m-1} + \mathbf{x}_m^T\mathbf{x}_m\right)\mathbf{w}_m\right. \\
&\left.+\mathbf{x}_m\left(y_m - \mathbf{w}_m\mathbf{x}_m\right)\right] \\
&= G_m\mathbf{w}_m - \mathbf{x}_m e_m \\
\Rightarrow G_m^{-1}\sum_{i=0}^{m} y_i\mathbf{x}_i &= \mathbf{w}_m - G_m^{-1}\mathbf{x}_m e_m \\
\Rightarrow \mathbf{w}_{m+1} &= \mathbf{w}_m - G_m^{-1}\mathbf{x}_m e_m
\end{aligned} \tag{11}$$

Then, the unscented Kalman filter is the adapting of the weights $\mathbf{w}_{m+1}$ represented as:

$$\mathbf{w}_{m+1} = \mathbf{w}_m - P_m\mathbf{x}_m e_m \tag{12}$$

$P_m = G_m^{-1}$ represents the speed which is not part of the model, but it is employed to find a solution, if $P_m$ is big we do not reach a convergence, and if $P_m$ is small we will reach a slow convergence. $\mathbf{w}_{m+1}$ represents the weights (2), (7) for iteration $m+1$, $\mathbf{w}_m$ represents the weights (2), (7) for iteration $m$, $\mathbf{x}_m$ represents the examples (2) for iteration $m$, and $e_m$ represents the error (3) for iteration $m$.

From the definition (8), we make operations to reach:

$$\begin{aligned}
G_m &= \sum_{i=0}^{m-1} \mathbf{x}_i^T\mathbf{x}_i + \mathbf{x}_m^T\mathbf{x}_m \\
&= G_{m-1} + \mathbf{x}_m^T\mathbf{x}_m
\end{aligned} \tag{13}$$

From (13), $P_m = G_m^{-1}$, and we use the inverse matrix lemma to reach:

$$\begin{aligned}
G_m^{-1} &= \left(G_{m-1} + \mathbf{x}_m^T\mathbf{x}_m\right)^{-1} \\
&= G_{m-1}^{-1} - \frac{1}{1+\mathbf{x}_m^T G_{m-1}^{-1}\mathbf{x}_m} G_{m-1}^{-1}\mathbf{x}_m\mathbf{x}_m^T G_{m-1}^{-1} \\
\Rightarrow P_m &= P_{m-1} - \frac{1}{1+\mathbf{x}_m^T P_{m-1}\mathbf{x}_m} P_{m-1}\mathbf{x}_m\mathbf{x}_m^T P_{m-1}
\end{aligned} \tag{14}$$

Then, we find the equation to update the speed:

$$P_m = P_{m-1} - \frac{1}{1+\mathbf{x}_m^T P_{m-1}\mathbf{x}_m} P_{m-1}\mathbf{x}_m\mathbf{x}_m^T P_{m-1} \tag{15}$$

$P_m = G_m^{-1}$.

From (2), (3), (12), and (15), the unscented Kalman filter is [18–20]:

$$\begin{aligned} \widehat{\mathbf{y}}_m &= \mathbf{w}_m \mathbf{x}_m \\ e_m &= \widehat{\mathbf{y}}_m - y_m \\ P_m &= P_{m-1} - \frac{1}{1+\mathbf{x}_m^T P_{m-1} \mathbf{x}_m} P_{m-1} \mathbf{x}_m \mathbf{x}_m^T P_{m-1} \\ \mathbf{w}_{m+1} &= \mathbf{w}_m - P_m \mathbf{x}_m e_m \end{aligned} \tag{16}$$

$P_m$ represents the speed, $e_m$ represents the error, $y_m$ represents the output, $\widehat{\mathbf{y}}_m$ represents the approximation output, $\mathbf{x}_m$ represents the examples, and $\mathbf{w}_m$ represents the weights.

## 3. Case 1: Orange solar drying

### 3.1. Model of the solar drying

The ability to approximate the behavior of food drying using solar energy can help producers to change parameters in their production methods. The orange, is a fruit rich in vitamin C and essential oils, its pulp is typically formed of eleven segments of juice filled with flavor goes from sweet to acid. One of the varieties of orange grown in Mexico is the valence. In 2014 citrus harvest was four million tons, which placed Mexico as the fourth largest producer in the world. A solar dryer with tracking process was built for this research. Several tests were conducted in July and October 2015. A model is proposed and compared with real data. A model is applied to approximate the behavior of the drying process.

The most abundant component in food is water. Determining the moisture content in food is one of the most important parts of the model which indicates the amount of water involved in the composition thereof. Values of moisture content in all samples became dimensionless, assuming the final moisture content is the equilibrium moisture content.

The moisture ratio $M_R$, as dimensionless moisture content can be calculated according to:

$$M_R = \frac{M_t - M_e}{M_0 - M_e} \tag{17}$$

$M_0$, $M_t$ and $M_e$ are the initial moisture content, the moisture content, and the equilibrium moisture content, respectively. The equilibrium moisture content is extremely small compared to the moisture content, then the equilibrium moisture content can be omitted. Different models which represent this process from experimental data are shown in Table 1.

Table 1
Models for the drying process

| Model | Equation |
|---|---|
| Page [21] | $MR = e^{-kt^n}$ |
| Newton [22] | $MR = e^{-kt}$ |
| Modified Page [23] | $MR = e^{-(kt)^n}$ |
| Exponential [24] | $MR = ae^{-kt}$ |
| Logarithmic [25] | $MR = ae^{-kt} + c$ |

One of the models used to determine the moisture content of agricultural products during the drying process is the exponential model, which from Newton's Law of Cooling, we have:

$$\dot{Q} = \alpha A(T - T_a) \tag{18}$$

$\alpha$ is the exchange heat coefficient, $A$ is the product area, $T$ is the product temperature, and $T_a$ is the ambient temperature. Furthermore, if a small amount of heat $dQ$ is transferred between a process with mass $m$ and its environment, the process undergoes a small change of temperature $dT$, then the specific heat capacity is defined as $c$, the model is:

$$c = \frac{1}{m}\frac{dQ}{dT} \tag{19}$$

Then,

$$mc\frac{dT}{dt} = \alpha A(T - T_a)$$

Simplifying,

$$\dot{T} = k(T(t) - T_a) \tag{20}$$

In which $k = \frac{\alpha A}{mc}$ is a proportionality constant. As it is assumed that the product is cooling, the process must satisfy $T > T_a$ and $k < 0$. If $T_0 = T(t = 0) \neq T_a$, then:

$$\dot{T} = k(T(t) - T_a) \neq 0$$

Consequently, there are no temperature variation. If $k > 0$ and $T_0 > T_a$ then $\dot{T} > 0$, then the temperature increases and the constant $k$ is negative, rewriting (20) for this case:

$$\dot{T} = -k(T(t) - T_a)$$

Thus, (20) with initial conditions is rewritten as:

$$\dot{T} = -k(T(t) - T_a), T(0) = T_0 \tag{21}$$

A solution of (21) is a function $T(t)$ which lets its satisfaction. First, we must find a function $T(t)$ as a solution of $\dot{T} = -k(T(t) - T_a)$. We must find

functions whose derivative is the product of $-k$ and $T(t) - T_a$. If:

$$P(t) = T(t) - T_a$$

Then,

$$\dot{P} = \dot{T}$$

We must be able to find a solution of (21) if we a find solution of $\dot{P} = -kP(t)$, and vice versa. If $P(t)$ is a solution of $\dot{P} = -kP(t)$ then $\dot{P}(t) = -kP(t)$. But $\dot{P}(t) = \dot{T}(t)$, $\dot{T}(t) = -kP(t) = -k(T(t) - T_a)$, then $T(t)$ is a solution of (21), and vice versa, if $T(t)$ is a solution of $\dot{P} = -kP(t)$, then as $\dot{P} = \dot{T}$ we have $\dot{P}(t) = \dot{T}(t) = -k(T(t) - T_a) = -kP(t)$.

Now, it is easier to find a solution of $\dot{P} = -kP(t)$ because we need to find a function whose derivative match. We know that a function that satisfies this property is the exponential function. Consequently, if $x(t) = e^t$ then $\dot{x}(t) = e^t = x(t)$. This means that $x(t) = e^t$ is a solution of $\dot{x} = x(t)$.

If we define $x(t) = e^{at}$ we have $\dot{x}(t) = ae^{at} = ax(t)$, then:

$$P(t) = e^{-kt} \tag{22}$$

$P(t)$ is a solution of $\dot{P} = -kP(t)$. Thus $\dot{P} = -ke^{-kt} = -kP(t)$. This is not a unique solution because if $P(t) = ce^{-kt}$ where $c$ is a constant, then $\dot{P}(t) = c(-ke^{-kt}) = -k(ce^{-kt}) = -kP(t)$. So $\dot{P}(t) = -kP(t)$. Then we conclude that:

$$M_R = P(t) = ce^{-kt} \tag{23}$$

To evaluate the fit of the model with the experimental data, the next statistical coefficients is used: chi-squared distribution $\chi^2$, mean squared error $MSE$, and root mean square error $RMSE$. Those are represented by:

$$\chi^2 = \frac{\sum_{i=1}^{N} \left(M_{R_{\exp,i}} - M_{R_{pre,i}}\right)^2}{N - z} \tag{24}$$

$$MSE = \frac{1}{N} \sum_{i=1}^{N} \left(M_{R_{pre,i}} - M_{R_{\exp,i}}\right)^2 \tag{25}$$

$$RMSE = \sqrt{\frac{1}{N} \sum_{i=1}^{N} \left(M_{R_{pre,i}} - M_{R_{\exp,i}}\right)^2} \tag{26}$$

$M_{R_{\exp,i}}$ represents the moisture ratio which is gotten experimentally, $M_{R_{pre,i}}$ are the approximations made by models, $N$ is the number of data, and $z$ is the number of constants.

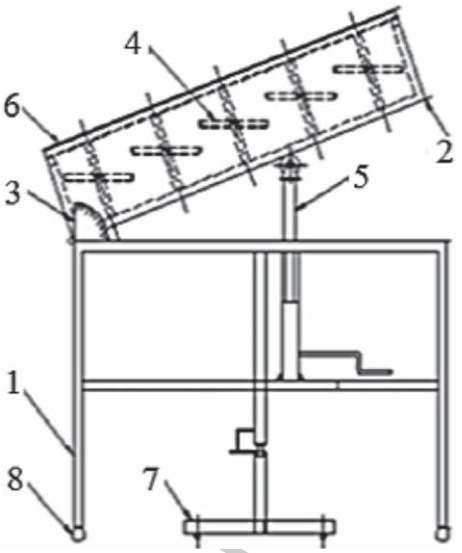


Fig. 1. Grading process.

The solar radiation that reach the ground on a horizontal surface is formed by direct radiation and diffuse radiation which together form the global solar radiation, their units are $\frac{\mathrm{W}}{\mathrm{m}^2}$ [3]. To obtain the global solar radiation we have used a pyranometer EPPLEY 8-48, which has a constant of $9.60 \times 10^{-6} \frac{\mathrm{W}}{\mathrm{m}^2}$.

### 3.2. Experimental prototype of solar drying

The prototype is built and presented in Fig. 2 where 4 are trays, 5 is the mechanical elevator, 6 are covers, 7 is the pivot base, and 8 are castors. The solar dryer with tracking process is a direct type dryers which operates by natural convection. The dimensions of the drying chamber are 300mm × 600mm × 1300mm, and it contains five trays constructed of 22 gauge galvanized sheet. On the upper surface it has two decks of clear glass with thick of 3mm, with a spacing between them of 50mm. The inclination of the drying chamber is $30^o$C to the horizontal plane and is oriented south-north to capture maximum solar energy.

The experimental test is: the orange used for drying tests are orange-valence type, which are being slicedwith about 5mm thickness and placed in each of the five trays on the drying chamber.

Each of the tests are conducted for a period of 12.5 hours, the hours in which tests are conducted were from 7:00 hours to 19:30 hours. In this period of time the data is gotten at intervals of 5 seconds, four temperatures are gotten at the same time: the ambient

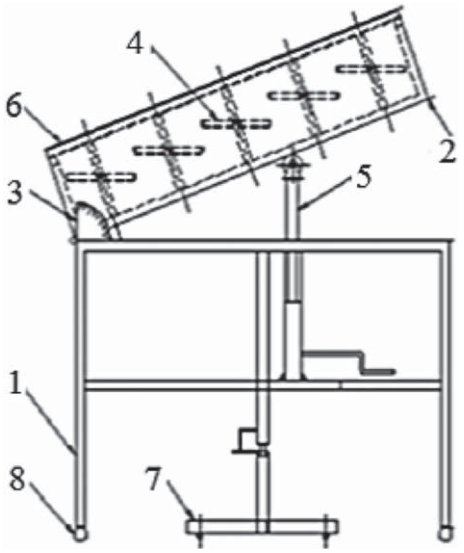


Fig. 2. Grading process.

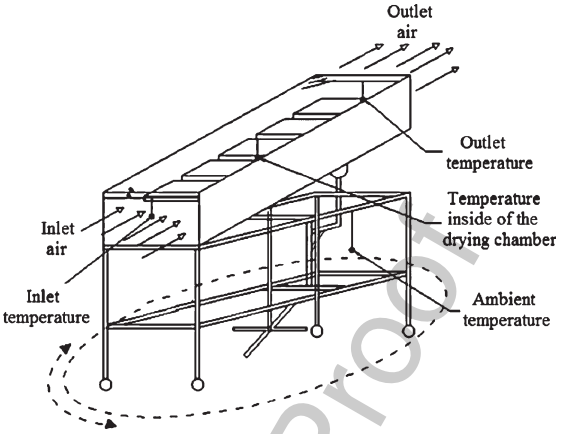


Fig. 3. Temperatures in the solar dryer prototype with tracking process.

Fig. 4. Experimental test with slices of orange inside.

temperature, inlet temperature of the drying chamber, temperature inside of the drying chamber, and outlet temperature of the drying chamber. Also, global radiation is recorded. Four temperatures are considered in the solar dryer, $T_1$ is the inlet temperature of the drying chamber, $T_2$ is the outlet temperature of the drying chamber, $T_3$ is the temperature inside the drying chamber, and $T_a$ is the ambient temperature, which are shown in Figs. 3 and 4.

The experimental test is: the orange used for drying tests are orange-valence type, which are being slicedwith about 5mm thickness and placed in each of the five trays on the drying chamber.

Each of the tests are conducted for a period of 12.5 hours, the hours in which tests are conducted were from 7:00 hours to 19:30 hours. In this period of time the data is gotten at intervals of 5 seconds, four temperatures are gotten at the same time: the ambient temperature, inlet temperature of the drying chamber, temperature inside of the drying chamber, and outlet temperature of the drying chamber. Also, global radiation is recorded. Four temperatures are considered in the solar dryer, $T_1$ is the inlet temperature of the drying chamber, $T_2$ is the outlet temperature of the drying chamber, $T_3$ is the temperature inside the drying chamber, and $T_a$ is the ambient temperature, which are shown in Figs. 3 and 4.

To evaluate moisture removal, the product mass is gotten in 10 seconds intervals. The average moisture content corresponding to the tests in July is of 55.746% and tests in October is of 52.906% of moisture removal. The data and results are presented in section Results.

## 4. Case 2: A greenhouse

### 4.1. Model of the greenhouse

For the model of crop growth, we represent the process as a model with four state variables, based on the work of [6]: $x_d$ is the crop dry weight in [kg m$^{-2}$], $x_c$ is the carbon dioxide concentration in [kg m$^{-3}$], $x_T$ is the air temperature in [$^{o}$C], and $x_h$ is the absolute humidity in [kg m$^{-3}$].

The representation of each of these variables is shown in (27), (29), (31), and (34).

$$\dot{x_d} = C_{\alpha\beta}\varphi_{phot,c} - C_{resp,d}x_d 2^{(0.1x_T - 2.5)} \quad (27)$$

Defining $C_{\alpha\beta} = C_\alpha C_\beta$ as the yield factor in which $C_\alpha$ corresponds to a factor that converts assimilated carbon dioxide into absorbed sugar equivalent, $C_\beta$ is a performance factor that counts synthesis and respiration losses during the conversion from carbohydrates to structure and whose value is between zero and one; as well as $\varphi_{phot,c}$ which is the photosynthesis rate in [kg m$^{-2}$ s$^{-1}$] represented in (28):

$$\varphi_{phot,c} = \left[\left(1 - e^{-C_{pl,d}x_d}\right) * \frac{C_{rad,phot}\nu_{rad}\left(-C_{co_{2,1}}x_T^2 + C_{co_{2,2}}x_T - C_{co_{2,3}}\right)(x_c - c_\Gamma)}{C_{rad,phot}\nu_{rad} + \left(-C_{co_{2,1}}x_T^2 + C_{co_{2,2}}x_T - C_{co_{2,3}}\right)(x_c - c_\Gamma)}\right] \quad (28)$$

Also $C_{pl,d}$ is the effective greenhouse surface in [m$^2$ kg$^{-1}$], $C_{rad,phot}$ is the light use efficiency in [kg J$^{-1}$], $\nu_{rad}$ is the solar radiation outside the greenhouse in [W m$^{-2}$], $C_{co_{2,1}}$ in [m s$^{-1}$ $^{o}$C$^{-2}$], $C_{co_{2,2}}$ in [m s$^{-1}$ $^{o}$C$^{-1}$], and $C_{co_{2,3}}$ in [m s$^{-1}$] represents the temperature influence on photosynthesis, $c_\Gamma$ is the carbon dioxide compensation point in [kg m$^{-3}$], $C_{resp,d}$ is the respiration rate expressed in terms of the amount of respired dry matter in [s$^{-1}$].

$$\dot{x_c} = \left[\frac{1}{C_{cap,c}} * \left(-\varphi_{phot,c} + C_{resp,c}x_d 2^{(0.1x_T - 2.5)} + u_c - \varphi_{vent,c}\right)\right] \quad (29)$$

Additionally, $C_{cap,c}$ is the greenhouse volume in [m], $C_{resp,c}$ is the respiration coefficient expressed in terms of the amount of carbon dioxide produced in [s$^{-1}$], $u_c$ is the supply rate of carbon dioxide in [kg m$^{-2}$ s$^{-1}$], $\varphi_{vent,c}$ is the mass exchange of carbon dioxide through the vents in [kg m$^{-2}$ s$^{-1}$], and is represented by (30).

$$\varphi_{vent,c} = (u_v + C_{leak})(x_c - \nu_c) \quad (30)$$

In which $u_v$ is the ventilation rate through the vents in [m s$^{-1}$], $C_{leak}$ is the leakage through the cover in [m s$^{-1}$], and $\nu_c$ is the carbon dioxide concentration outside the greenhouse in [kg m$^{-3}$].

$$\dot{x_T} = \frac{1}{C_{cap,q}}\left(u_q - Q_{vent,q} + Q_{rad,q}\right) \quad (31)$$

$C_{cap,q}$ is the heat capacity of the greenhouse air in [J m$^{-2}$ $^{o}$C$^{-1}$], $u_q$ is the energy supply by the heating process in [W m$^{-2}$], $Q_{vent,q}$ is the energy exchange with the outdoor air due the ventilation and transmission through the cover in [W m$^{-2}$] governed by (32), $Q_{rad,q}$ is the heat load due to the solar radiation in [W m$^{-2}$], and is expressed by (33).

$$Q_{vent,q} = \left(C_{cap,q,v}u_v + C_{ai,ou}\right)(x_T - \nu_T) \quad (32)$$

In which $C_{cap,q,v}$ is the heat capacity per volume unit of greenhouse air in [J m$^{-3}$ $^{o}$C$^{-1}$], $C_{ai,ou}$ represents the overall heat transfer through the cover in [W m$^{-2}$ $^{o}$C$^{-1}$], and $\nu_T$ is the outside air temperature in [$^{o}$C].

$$Q_{rad,q} = C_{rad,q}\nu_{rad} \quad (33)$$

$C_{rad,q}$ is the heat load coefficient due to solar radiation.

$$\dot{x_h} = \frac{1}{C_{cap,h}}\left(\varphi_{transp,h} - \varphi_{vent,h}\right) \quad (34)$$

In which $C_{cap,h}$ is the greenhouse volume in [m], $\varphi_{transp,h}$ is the transpiration in [kg m$^{-2}$ s$^{-1}$] represented in (35), and $\varphi_{vent,h}$ is the mass exchange of water vapor through the vents in [kg m$^{-2}$ s$^{-1}$].

$$\varphi_{transp,h} = \left[\left(1 - e^{-C_{pl,d}x_d}\right) * C_{v,pl,ai}\left(\frac{C_{v,1}}{C_R(x_T + C_{T,abs})}e^{\frac{C_{v,2}x_T}{x_T + C_{v,3}}} - x_h\right)\right] \quad (35)$$

The term $\frac{C_{v,1}}{C_R(x_T + C_{T,abs})}e^{\frac{C_{v,2}x_T}{x_T + C_{v,3}}}$ represents the saturated water vapor content at temperature $x_T$ in the upper region of the greenhouse in [kg m$^{-3}$], $C_{v,pl,ai}$ is the mass transfer coefficient in [m s$^{-1}$], $C_{v,1}$ in [J m$^{-3}$], $C_{v,2}$ and $C_{v,3}$ in [$^{o}$C] are values that represent the saturation water vapor pressure in the greenhouse, $C_R$ is the gas constant in [J K$^{-1}$ kmol$^{-1}$], $C_{T,abs}$ represents the conversion of temperature from $^{o}$C to $^{o}$K, $\varphi_{vent,h}$ is the mass exchange of water vapor through the vents in [kg m$^{-2}$ s$^{-1}$], which we represent by (36).

$$\varphi_{vent,h} = (u_v + C_{leak})(x_h - \nu_h) \quad (36)$$

$\nu_h$ is the humidity concentration outside the greenhouse in [kg m$^{-3}$].

If the state variables are defined as $x_1 = x_c$, $x_2 = x_T$, $x_3 = x_h$, $x_4 = x_d$, control inputs as $u_1 = u_c$, $u_2 = u_v$, $u_3 = u_q$, and functions as $f_a = \varphi_{phot,c}$, $f_b = 2^{(0.1x_T - 2.5)}$, $f_c = \varphi_{transp,h}$, then we rewrite (27), (29),

(31), (34) as:

$$\begin{aligned}
\dot{x_1} &= \left[\frac{1}{C_{cap,c}}(-f_a + C_{resp,c}x_4 f_b - C_{leak}(x_1 - v_c)) \right.\\
&\left. + \frac{1}{C_{cap,c}}u_1 - \frac{(x_1 - v_c)}{C_{cap,c}}u_2\right]\\
\dot{x_2} &= \left[\frac{1}{C_{cap,q}}\left(Q_{rad,q} - C_{ai,ou}\left(x_2 - v_T\right)\right)\right.\\
&\left. - \frac{C_{cap,qv}\left(x_2 - v_T\right)}{C_{cap,q}}u_2 + \frac{1}{C_{cap,q}}u_3\right]\\
\dot{x_3} &= \frac{1}{C_{cap,h}}\left(f_c - C_{leak}\left(x_3 - v_h\right)\right) - \frac{(x_3 - v_h)}{C_{cap,h}}u_2\\
\dot{x_4} &= C_{\alpha\beta}f_a - C_{resp,d}f_b x_4
\end{aligned} \tag{37}$$

With:

$$\begin{aligned}
f_a &= \left[\left(1 - \mathrm{e}^{-C_{pl,d}x_4}\right)\right.\\
&\left.*\frac{C_{rad,phot}v_{rad}\left(-C_{co_{2,1}}x_2^2 + C_{co_{2,2}}x_2 - C_{co_{2,3}}\right)(x_1 - c_\Gamma)}{C_{rad,phot}v_{rad} + \left(-C_{co_{2,1}}x_2^2 + C_{co_{2,2}}x_2 - C_{co_{2,3}}\right)(x_1 - c_\Gamma)}\right]\\
f_b &= 2^{(0.1x_2 - 2.5)}\\
f_c &= \left[\left(1 - \mathrm{e}^{-C_{pl,d}x_4}\right)\right.\\
&\left.*C_{v,pl,ai}\left(\frac{C_{v,1}}{C_R\left(x_2 + C_{T,abs}\right)}\mathrm{e}^{\frac{C_{v,2}x_2}{x_2 + C_{v,3}}} - x_3\right)\right]\\
Q_{rad,q} &= C_{rad,q}v_{rad}
\end{aligned}$$

Model parameters are listed in Table 2. Parameters of Table 2 represent the best values such that the model (37) represent in the best form a greenhouse, they were validated by experiments in [2, 6].

Table 2
Greenhouse parameters

| Parameter | Parameter |
|---|---|
| $C_{resp,d} = 2.65 \times 10^{-7}\mathrm{s}^{-1}$ | $C_{\alpha\beta} = 0.544$ |
| $C_{ai,ou} = 6.1\mathrm{Wm}^{-2o}\mathrm{C}^{-1}$ | $C_{rad,q} = 0.2$ |
| $c_\Gamma = 5.2 \times 10^{-5}\mathrm{kgm}^{-3}$ | $C_{T,abs} = 273.15\mathrm{K}$ |
| $C_{resp,c} = 4.87 \times 10^{-7}\mathrm{s}^{-1}$ | $C_{pl,d} = 53\mathrm{m}^2\mathrm{kg}^{-1}$ |
| $C_{cap,q} = 30000\mathrm{Jm}^{-2o}\mathrm{C}^{-1}$ | $C_{v,1} = 9348\mathrm{Jm}^{-3}$ |
| $C_{cap,q,v} = 1290\mathrm{Jm}^{-3o}\mathrm{C}^{-1}$ | $C_{v,2} = 17.4$ |
| $Cco_{2,1} = 5.11 \times 10^{-6}\mathrm{ms}^{-1o}\mathrm{C}^{-2}$ | $C_{v3} = 239^o\mathrm{C}$ |
| $Cco_{2,2} = 2.30 \times 10^{-4}\mathrm{ms}^{-1o}\mathrm{C}^{-2}$ | $C_{v4} = 10998\mathrm{Jm}^{-3}$ |
| $Cco_{2,3} = 6.29 \times 10^{-4}\mathrm{ms}^{-1}$ | $C_{cap,c} = 4.1\mathrm{m}$ |
| $C_{leak} = 0.75 \times 10^{-4}\mathrm{ms}^{-1}$ | $C_{cap,h} = 4.1\mathrm{m}$ |
| $x_{1\max} = 2.75 \times 10^{-3}\mathrm{Kgm}^{-3}$ | $x_{1\min} = 0\mathrm{Kgm}^{-3}$ |
| $C_R = 8314\mathrm{JK}^{-1}\mathrm{kmol}^{-1}$ | $x_{2\min} = 6.5^o\mathrm{C}$ |
| $C_{rad,phot} = 3.55 \times 10^{-9}\mathrm{kgJ}^{-1}$ | $x_{2\max} = 40^o\mathrm{C}$ |
| $C_{v,pl,ai} = 3.6 \times 10^{-3}\mathrm{ms}^{-1}$ | |

### 4.2. Experimental prototype of the greenhouse

The prototype of the is shown in Fig. 5. We represent the variables of the process in the past subsection.

### 4.3. State feedback control for the crop growth process

The model (37) can be expressed in matrix form according to [26, 27] as:

$$\begin{bmatrix}\dot{x}_1\\ \dot{x}_2\\ \dot{x}_3\\ \dot{x}_4\end{bmatrix} = \begin{bmatrix}A_1\\ A_2\\ A_3\\ A_4\end{bmatrix} + \begin{bmatrix}B_{11} & B_{12} & 0\\ 0 & B_{22} & B_{23}\\ 0 & B_{32} & 0\\ 0 & 0 & 0\end{bmatrix}\begin{bmatrix}u_1\\ u_2\\ u_3\end{bmatrix} \tag{38}$$

With:

$$\begin{aligned}
A_1 &= \frac{2^{0.1x_2 - 2.5}C_{resp,c}x_4 - C_{leak}(x_1 - v_c)}{C_{cap,c}} - \frac{\frac{A_{11n}}{A_{11d}}}{C_{cap,c}}\\
A_{11n} &= \left[\left(1 - e^{-C_{pl,d}x_4}\right)C_{rad,phot}\left(x_1 - c_\Gamma\right)\right.\\
&\left.*\left(-C_{co_{2,1}}x_2^2 + C_{co_{2,2}}x_2 - C_{co_{2,3}}\right)v_{rad}\right]\\
A_{11d} &= \left[C_{rad,phot}v_{rad}\right.\\
&\left.+ (x_1 - c_\Gamma)\left(-C_{co_{2,1}}x_2^2 + C_{co_{2,2}}x_2 - C_{co_{2,3}}\right)\right]\\
A_2 &= \frac{C_{rad,q}v_{rad} - C_{ai,ou}(x_2 - v_T)}{C_{cap,q}}\\
A_3 &= \frac{A_{33n}}{C_{cap,h}}\\
A_{33n} &= [-C_{leak}\left(x_3 - v_h\right)\\
&+ \left(1 - e^{-C_{pl,d}x_4}\right)C_{v,pl,ai}\left(\frac{e^{\frac{C_{v,2}x_2}{C_{v,3} + x_2}}C_{v,1}}{C_R(C_{T,abs} + x_2)} - x_3\right)\Bigg]\\
A_4 &= -2^{0.1x_2 - 2.5}C_{resp,d}x_4 + \frac{A_{44n}}{A_{44d}}\\
A_{44n} &= \left[\left(1 - e^{-C_{pl,d}x_4}\right)C_{rad,phot}C_{\alpha\beta}\left(x_1 - c_\Gamma\right)\right.\\
&\left.\left(-C_{co_{2,1}}x_2^2 + C_{co_{2,2}}x_2 - C_{co_{2,3}}\right)v_{rad}\right]\\
A_{44d} &= \left[C_{rad,phot}v_{rad}\right.\\
&\left.+ (x_1 - c_\Gamma)\left(-C_{co_{2,1}}x_2^2 + C_{co_{2,2}}x_2 - C_{co_{2,3}}\right)\right]\\
B_{11} &= \frac{1}{C_{cap,c}},\ B_{12} = -\frac{(x_1 - v_c)}{C_{cap,c}},\\
B_{22} &= -\frac{C_{cap,qv}(x_2 - v_T)}{C_{cap,q}}\\
B_{23} &= \frac{1}{C_{cap,q}},\ B_{32} = -\frac{(x_3 - v_h)}{C_{cap,h}}
\end{aligned} \tag{39}$$

For the nonlinear model (39), we employ a control law as:

$$u = \left[B^{\mathrm{T}}B\right]^{-1}B^{\mathrm{T}}\left[-A + \dot{x_s} - \frac{1}{2}k_s\mathrm{e}_s\right] \tag{40}$$

$\mathrm{e}_s = x - x_s$, $k_s$ represents a positive constant, $u = \left[u_1\ u_2\ u_3\right]^T$ represents the input. We employ the

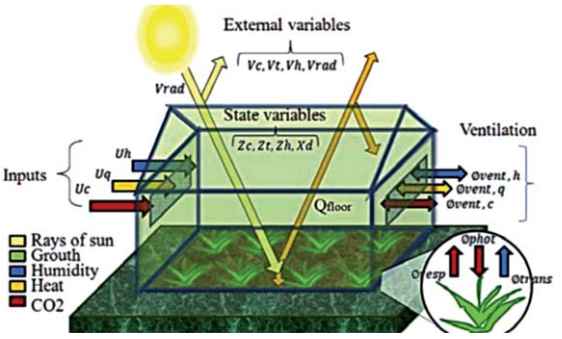


Fig. 5. Prototype of the greenhouse.

state feedback control to reach $\dot{e_s} = -\frac{1}{2}k_s e_s$. If (40) is replaced in (38), (39), then the tracking error of closed loop process of the state feedback control applied to the nonlinear process is exponentially convergent $\dot{e_s} = -\frac{1}{2}k_s e_s$ [26, 28]. If we define the Lyapunov functions as $v_s = \frac{1}{2}e_s^T$ and solve de derivative of $v_s$ as $\dot{v_s} = e_s^T \dot{e_s} = -\frac{1}{2}k_s e_s^T = -k_s v_s$, the solution is $v_s = e^{-k_s t} v_{si}$, in which $v_{si}$ is the initial condition of $v_s$, which can be expressed as $v_s = e^{-k_s t} v_{si} = \frac{1}{2}e^{-k_s t} \parallel e_{si} \parallel^2$, where $e_{si}$ is the initial condition of the tracking error $e_s$.

## 5. Results

In this section, the unscented Kalman filter (16) is applied for the experimental learning of the next two processes: a solar dryer for oranges drying and a greenhouse for crop growth. The unscented Kalman filter of (16) called Unscented Kalman Filter is compared with the extreme machine learning of [11] called Machine Learning 1 and with the extreme learning machine of [12] called Machine Learning 2. We compare the data of $y_m$ with $\widehat{\mathbf{y}}_m$. We use the determination coefficient $R^2$, it is a parameter which determines the quality of the experimental learning:

$$R^2 = 1 - \frac{\sum_{mf} \left(\widehat{\mathbf{y}}_m - \overline{y}_m\right)^2}{\sum_{mf} \left(y_m - \overline{y}_m\right)^2} \tag{41}$$

$\widehat{\mathbf{y}}_m$ represents the approximation output, $y_m$ represents the output, $\overline{y}_m$ represents the mean of the output $y_m$, and $mf$ represents the final time. $R^2$ generates values from 0 to 1. If an algorithm has good performance $R^2$ has values near to 1, and if an algorithm has bad performance $R^2$ has values near to 0.

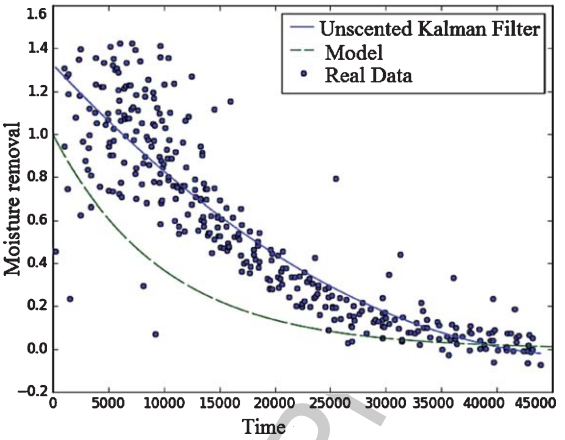


Fig. 6. Comparison between the unscented Kalman filter and a model for the learning of orange drying.

### 5.1. Learning of the solar drying

Temperatures $T_1, T_2, T_3, T_a$ are renamed as $\mathbf{x}_1, \mathbf{x}_2, \mathbf{x}_3, \mathbf{x}_4$. Those features affect the drying behavior $M_R$ renamed as $\mathbf{y}$. Dataset from sensors has 8000 lectures covering 12.5 hours from 7:00 to 19:30 during a sunny day. It is desired the experimental learning during the drying process $\hat{\mathbf{y}}$ using an hypothesis to define the necessary parameters to have an acceptable drying process.

In Fig. 6 we represent the results found for the average percentage of moisture removal on drying orange slices with dimensionless units versus the time in seconds, equivalent to each one of the five tests conducted using $c = 59.243$, $k = 0.411$, $\chi^2 = 0.00067$, $MSE = 0.994$, and $RMSE = 0.010$ for the model, in which $c$ represents the higher percentage of moisture removal on all tests and $k$ represents a constant offset for fitting. In the Unscented Kalman Filter, we employ the speed $\alpha = 0.01$ and a total of 1000 iterations. We apply several near values of the initial conditions in the unscented Kalman filter as shown in Fig. 7.

The comparison of the Unscented Kalman Filter, Machine Learning 1, and Machine Learning 2 is show in the Table 3 for the $R^2$ of equation (41).

Fig. 7 and Table 3 yield that the that the Unscented Kalman Filter reaches better learning than both Machile Learning 1 and Machile Learning 2 due to the Unscented Kalman filter obtains the biggest $R^2$.

### 5.2. Learning of the greenhouse

The state variables carbon dioxide concentration $\mathbf{x}_1$, air temperature $\mathbf{x}_2$, and absolute humidity inside

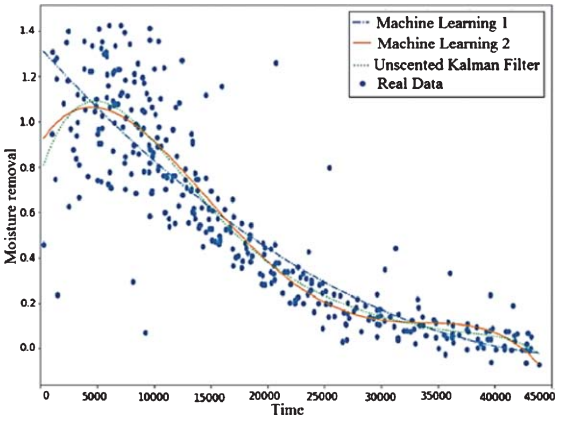


Fig. 7. Unscented Kalman filter for the learning of orange drying.

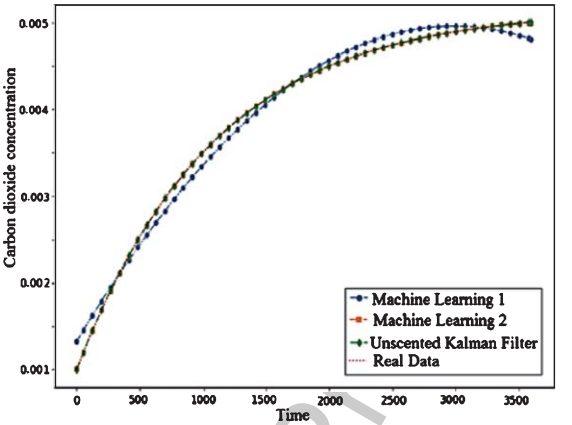


Fig. 8. Unscented Kalman filter for the learning of carbon dioxide concentration.

Table 3
Comparison results

| | $R^2$ |
|---|---|
| Machine Learning 1 | 0.9020 |
| Machine Learning 2 | 0.9217 |
| Unscented Kalman Filter | 0.9314 |

Table 4
Comparison results

| | $R^2$ |
|---|---|
| Machine Learning 1 | 0.9141 |
| Machine Learning 2 | 0.9314 |
| Unscented Kalman Filter | 0.9420 |

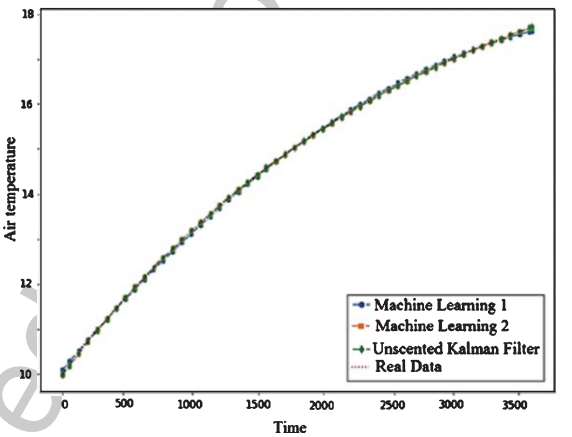


Fig. 9. Unscented Kalman filter for the learning of air temperature.

the greenhouse $\mathbf{x}_3$ affect the behavior of the crop dry weight $\mathbf{y}$. It is desired the experimental learning during the crop growth $\hat{\mathbf{y}}$ the using a hypothesis to define the necessary parameters to have an acceptable harvest.

Taking the data and using the Unscented Kalman Filter make possible the experimental learning of the behavior of the carbon dioxide concentration in [kg m$^{-3}$], the air temperature in [°C], and the absolute humidity in [kg m$^{-3}$] inside the greenhouse versus the time in seconds as shown in Figs. 8–10, respectively.

The comparison of the Unscented Kalman Filter, Machine Learning 1, and Machine Learning 2 is show in the Table 4 for the $R^2$ of equation (41).

Figures 8–10, and Table 4 yield that the that the Unscented Kalman Filter reaches better learning than both Machile Learning 1 and Machile Learning 2 due to the Unscented Kalman filter obtains the biggest $R^2$.

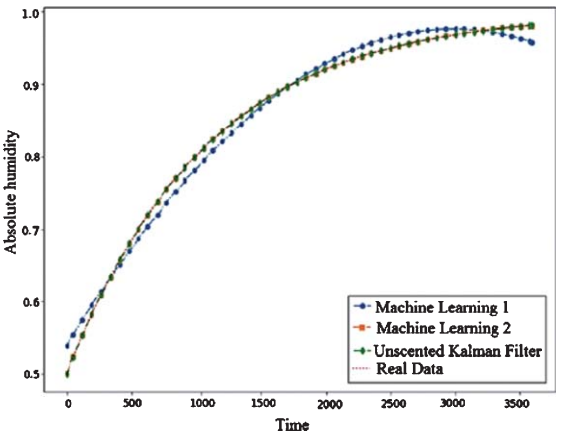


Fig. 10. Unscented Kalman filter for the learning of absolute humidity.

## 6. Conclusions

The results gotten in this document show that it is possible to dry orange slices using a direct type solar dryer through natural convection, earning up to 59.243% moisture removal of the product in a time of six hours. A model represented accurately the drying process with a success of 84%. The unscented Kalman filter was programmed for the experimental learning of the behavior during the drying process of orange slices with a success of 0.93. Furthermore, the unscented Kalman filter was programmed for the experimental learning of the behavior during the crop growth with a success of 0.94. In the forthcoming work, other alternative algorithms for the experimental learning will be designed, and other physical processes will be studied.

## Acknowledgment

The authors are grateful to the editors and reviewers for their valuable comments and insightful suggestions, which helped to improve this research significantly. The authors thank the Instituto Politécnico Nacional, the Secretaría de Investigación y Posgrado, Comisión de Operación y Fomento de Actividades Académicas, and Consejo Nacional de Ciencia y Tecnología for their help in this study.

## References

[1] J.L. Mendoza-Medina, G. Martínez-Soto, M.L. Alcántara-González, M. López-Orozco and J. Mercado-Flores, Modelos aplicados al proceso de secado del chile poblano. VII Congreso Nacional de Ciencia de los Alimentos y III Foro de Ciencia y Tecnología de Alimentos, Guanajuato, Gto, 2003, pp. 416-424.

[2] V. Henten, Greenhouse climate management, an optimal control approach, Tesis doctoral. Wageningen Agricultural University, Netherlands, 1994.

[3] Y. Mghouchi, A. Bouardi, Z. Choulli and T. Ajzoul, Models for obtaining the daily direct, diffuse and global solar radiations, *Renewable and Sustainable Energy Reviews* **56** (2016), 87–99.

[4] B.A. Eke, Development of small scale direct mode natural convection solar dryer for tomato, okra and carrot, *International Journal of Engineering and Technology* **3**(2) (2013), 199–204.

[5] H. Chen, C.E. Hernandez and T. Huang, A study of the drying effect on lemon slices using a closed-type solar dryer, *Solar Energy* **78** (2005), 97–103.

[6] J.J. Rubio, G. Gutierrez, J. Pacheco and H. Perez, Comparison of three proposed controls to accelerate the growth of crop, *International Journal of Innovative Computing, Information and Control* **7** (2011), 4097–4114.

[7] L. Duan, M. Xie, J. Wang and T. Bai, Deep learning enabled intelligent fault diagnosis: Overview and applications, *Journal of Intelligent & Fuzzy Systems* **35**(5) (2018), 5771–5784.

[8] S.-H. Lee and M.-S. Kang, Intelligent noise prediction scheme with pattern analysis and deep learning technique, *Journal of Intelligent & Fuzzy Systems* **35**(6) (2018), 5867–5879.

[9] Y. Narayan, L. Mathew and S. Chatterji, sEMG signal classification with novel feature extraction using different machine learning approaches, *Journal of Intelligent & Fuzzy Systems* **35**(5) (2018), 5099–5109.

[10] T.O. Owolabi and M.A. Gondal, Quantitative analysis of LIBS spectra using hybrid chemometric models through fusion of extreme learning machines and support vector regression, *Journal of Intelligent & Fuzzy Systems* **35**(6) (2018), 6277–6286.

[11] A.G.C. Pacheco, R.A. Krohling and C.A.S. da Silva, Restricted Boltzmann machine to determine the input weights for extreme learning machines, *Expert Systems With Applications* **96** (2018), 77–85.

[12] M. Uzair, F. Shafait, B. Ghanem and A. Mian, Representation learning with deep extreme learning machines for efficient image set classification, *Neural Computing & Applications* **30** (2018), 1211–1223.

[13] A. Kukker and R. Sharma, Neural reinforcement learning classifier for elbow, finger and hand movements, *Journal of Intelligent & Fuzzy Systems* **35**(5) (2018), 5111–5121.

[14] R. Tiwari, M.K. Saxena, P. Mehendiratta, K. Vatsa, S. Srivastava and R. Gera, Market segmentation using supervised and unsupervised learning techniques for E-commerce applications, *Journal of Intelligent & Fuzzy Systems* **35**(5) (2018), 5353–5363.

[15] J.J. Rubio, E. Lughofer, J.A. Meda-Campaña, L.A. Paramo, J.F. Novoa and J. Pacheco, Neural network updating via argument Kalman filter for modeling of Takagi-Sugeno fuzzy models, *Journal of Intelligent & Fuzzy Systems* **35**(2) (2018), 2585–2596.

[16] J.J. Rubio, Stable Kalman filter and neural network for the chaotic systems identification, *Journal of the Franklin Institute* **354**(16) (2017), 7444–7462.

[17] S. Yousefizadeh, J.D. Bendtsen, N. Vafamand, M.H. Khooban, T. Dragicevic and F. Blaabjerg, EKF-based predictive stabilization of shipboard DC microgrids with uncertain time-varying load, *IEEE Journal of Emerging and Selected Topics in Power Electronics* **7**(2) (2019), 901–909.

[18] B. Safarinejadian and N. Vafamand, Kalman randomized joint UKF algorithm for dual estimation of states and parameters in a nonlinear system, *Journal of Electrical Engineering & Technology* **10** (2015), 742–750.

[19] N. Vafamand, M.M. Arefi and A. Khayatian, Nonlinear system identification based on Takagi-Sugeno fuzzy modeling and unscented Kalman filter, *ISA Transactions* **74** (2018), 134–143.

[20] M.A. Kardan, M.H. Asemani, A. Khayatian, N. Vafamand, M.H. Khooban, T. Dragicevic and F. Blaabjerg, Improved stabilization of nonlinear DC microgrids, cubature kalman filter approach, *IEEE Transactions on Industry Applications* **54**(5) (2018), 5104–5112.

[21] Y.C. Agrawal and R.D. Singh, Thin layer drying studies for short grain rice, *Journal of Agricultural Engineering* **21** (1977), 41–47.

[22] J.R. O'Callaghan, D.J. Menzies and P.H. Bailey, Digital simulation of agricultural drier performance, *Journal of Agricultural Engineering Research* **16** (1971), 223–244.

[23] D.G. Overhults, G.M. White, H.E. Hamilton and I.J. Ross, Drying soybeans with heated air, *Transactions of the ASAE* **16** (1973), 112–113.
[24] P.W. Westerman, G.M. White and I.J. Ross, Relative humidity effect on the high-temperature drying of shelled corn, *Transactions of the ASAE* **16** (1973), 1136–1139.
[25] S.M. Henderson, Progress in developing the thin layer drying equation, *Transactions of the ASAE* **16** (1974), 1167–1168.
[26] H.K. Khalil, Nonlinear systems, Prentice Hall, 3ra Edición, 2002.
[27] J.E. Slotine and W. Li, Applied nonlinear control, MacMillan, 1991.
[28] P.A. Ioannou and J. Sun, Robust adaptative control, Prentice Hall, 1996.